International Journal of Nanomedicine

Dovepress
open access to scientific and medical research

Open Access Full Text Article

ORIGINAL RESEARCH

Preparation, characterizations and anti-pollutant activity of 7,3′,4′-trihydroxyisoflavone nanoparticles in particulate matter-induced HaCaT keratinocytes

This article was published in the following Dove Press journal:
International Journal of Nanomedicine

Pao-Hsien Huang[1]
Chih-Hua Tseng[1]
Chia-Yu Lin[2]
Chiang-Wen Lee[3–5]
Feng-Lin Yen[2,6]

[1]School of Pharmacy, [2]Department of Fragrance and Cosmetic Science, College of Pharmacy, Kaohsiung Medical University, Kaohsiung, [3]Research Center for Industry of Human Ecology, Chang Gung University of Science and Technology, Kweishan, Taoyuan, [4]Department of Nursing, Division of Basic Medical Sciences, [5]Chronic Diseases and Health Promotion Research Center, Chang Gung University of Science and Technology, Chia-Yi, [6]Institute of Biomedical Sciences, National Sun Yat-Sen University, Kaohsiung, Taiwan, Republic of China

Background: 7,3′,4′-Trihydroxyisoflavone (734THI), a secondary metabolite derived from daidzein in soybean, possesses several biological activities, including antioxidant, skin whitening and anti-atopic dermatitis properties, but the poor aqueous solubility of 734THI has limited its application in medicine and cosmetic industry.

Methods: The aim of the present study was to improve the physicochemical properties of 734THI using planetary ball mill preparation under a solvent-free process to improve its solubility and anti-pollutant activity.

Results: 734THI nanoparticle powder (734THIN) was successfully prepared by the planetary ball mill technique using polyvinylpyrrolidone K30 as the excipient. 734THIN effectively increased the aqueous solubility and cellular uptake of 734THI by improving its physicochemical properties, including particle size reduction, crystalline–amorphous transformation and intermolecular hydrogen bonding with polyvinylpyrrolidone K30. In addition, 734THIN inhibited the overexpression of COX-2 and MMP-9 by downregulating MAPK pathway signaling in particulate matter-exposed HaCaT keratinocytes, while raw 734THI in PBS with low aqueous solubility did not show any anti-inflammatory or antiaging activity.

Conclusion: 734THIN may be used as an additive in anti-pollutant skin care products for preventing particulate matter-induced inflammation and aging in skin.

Keywords: 7,3′,4′-trihydroxyisoflavone, nanoparticle, planetary ball mill, particulate matter, inflammation

Introduction

Atmospheric pollutants, including particulate matter (PM), gases, polycyclic aromatic hydrocarbons, volatile organic compounds, oxides, ozone and cigarette smoke, are a major public health concern. PM can easily contact the barriers of the human body and exert deleterious effects on the eyes, ears, nose and skin. The skin is the largest and outermost organ of the human body, and PM can directly penetrate the skin barrier and enter the subcutaneous tissue through skin appendages, including hair follicles, sweat glands and sebaceous glands. Previous studies have indicated that PM can induce oxidative stress, skin barrier function impairment and immune injury of the skin, and lead to many dermatological disorders including dry skin, rashes, dermatitis, inflammation, alopecia, progressive loss of skin integrity and aging.[1] Accordingly, dietary supplements containing antioxidants, such as *N*-acetylcysteine,[2] can prevent the development of alopecia. In addition, caffeic acid phenethyl ester,[3] dehydroepiandrosterone[4] and resveratrol[5] can reduce reactive oxygen species production and inflammatory responses to prevent PM-induced skin diseases.

Correspondence: Feng-Lin Yen
Department of Fragrance and Cosmetic Science, College of Pharmacy, Kaohsiung Medical University, 100 Shih-Chuan 1st Road, Kaohsiung 807, Taiwan
Tel +886 7 312 1101 ext 2028
Fax +886 7 321 0683
Email flyen@kmu.edu.tw

submit your manuscript | www.dovepress.com
Dovepress
http://dx.doi.org/10.2147/IJN.S153323

Daidzin and Genistin are glycosides, and their aglycones are daidzein and genistein. These isoflavones are the naturally occurring dietary phytoestrogens distributed in soybean.[6] It is well known that soybean isoflavones possess anti-cancer, antioxidant, antiangiogenic, anti-inflammatory and anti-estrogenic activities. In the past few decades, extensive studies in the fields of dermatology and cosmetology have demonstrated that soybean isoflavones, such as genistein and 7,3′,4′-trihydroxyisoflavone (734THI), could be effective anti-atopic dermatitis,[7] anti-melanoma[8] and skin whitening[9] agents for skin care. However, the anti-pollutant activity of 734THI has not been investigated previously.

According to the biopharmaceutical classification system (BCS) from the US Food and Drug Administration, many poorly soluble drugs are classified as class II (low aqueous solubility and high permeability) or IV (low aqueous solubility and low permeability) drugs.[10] The physicochemical properties of poorly soluble drugs may lead to low absorption, which may limit their application in medicine and in the cosmetic industry.[11] In recent years, several techniques have been described to enhance the aqueous solubility and dissolution rate of drugs, and thereby improve their bioavailability, including hot melt extrusion,[12,13] spray drying,[14] salt formation,[15] solid dispersion,[16] hydrogel microparticles[17] and size reduction.[18] Nanoparticle technology is one of the size reduction methods such as co-grinding and nanoprecipitation. Previous studies have demonstrated that ball mill technology (BMT) is an easy, effective and novel co-grinding method, which has been used for drugs such as nifedipine,[19] indomethacin[20] and griseofulvin.[21] BMT is often applied to prepare nanoparticle powders because of its quickness, fineness and reproducibility. Planetary ball mill is a novel BMT and few studies have used this technique to prepare nanoparticle powder from poorly soluble drugs or natural medicines. Thus, this technique will be investigated in the present study.

The aqueous solubility of 734THI is about 20 μg/mL, which indicates that 734THI belongs to BCS class II. The anti-pollutant activities of 734THI and its nanoparticle formulation have not been investigated previously. Moreover, pharmaceutical excipients have been employed to improve the solubility of poorly water soluble drugs for various topical preparations, oral suspensions and solutions. Polyvinylpyrrolidone (PVP) is one of the excipients commonly used to prepare nanoparticle formulations because of its suspending, stabilizing and anti-plasticizing effects.[22] Consequently, PVP was chosen to prepare the nanoparticle formulation in the present study. The purpose of the present study was to improve the aqueous solubility and cellular uptake of 734THI by nanoparticle formulation using planetary BMT. The physicochemical properties of raw 734THI and its nanoparticle powder were characterized using scanning electron microscopy (SEM), transmission electron microscopy analysis (TEM), powder X-ray diffractometry (XRD) and Fourier transformation infrared spectroscopy (FT-IR). We also used Western blotting assay to determine the expression of proteins involved in inflammation and aging, in order to compare the anti-pollutant activity of raw 734THI and its nanoparticle powder.

Materials and methods

Materials

734THI was synthesized by Assistant Professor Chih-Hua Tseng, College of Pharmacy, Kaohsiung Medical University. PVP K30 (average molecular weight 40,000, K-value 29–32), dimethyl sulfoxide (DMSO) and DMSO-*d6* were obtained from Sigma (St Louis, MO, USA). The HaCaT keratinocyte cell line was supplied by Professor Jeff Yi-Fu Chen, Department of Biotechnology, Kaohsiung Medical University. DMEM/F12 was obtained from Thermo Fisher Scientific (Waltham, MA, USA). PM (Standard Reference Material® 1649b) was purchased from the National Institute of Standards and Technology (Gaithersburg, MD, USA). Primary antibodies, COX-2, ICAM, MMP-9, GAPDH and HRP-conjugated goat anti-rabbit IgG antibodies, were obtained from Santa Cruz Biotechnology (Dallas, TX, USA). cPLA2, phospho-ERK, phospho-p38 and phospho-JNK antibodies were purchased from Cell Signaling (Danvers, MA, USA). All other chemical reagents were of analytical grade.

Synthesis of 734THI

The synthesis of 734THI was performed as described previously.[23] Briefly, resorcinol (0.05 M) and 3,4-dihydroxy phenylacetic acid (0.05 M) were dissolved in freshly distilled boron trifluoride diethyl etherate under argon. The mixture was then stirred and heated to 80°C. The corresponding intermediate product 1-(2,4-dihydroxyphenyl)-2-(3,4-dihydroxyphenyl)ethanone was isolated by thorough washing of the collected material with sodium acetate aqueous solution and ethyl acetate. Purification of the residue by column chromatography on silica gel was performed using a mixture of dichloromethane and methanol. Freshly distilled boron trifluoride diethyl etherate (6.3 mL) was added under argon to a solution of the intermediate product (520 mg, 2 mM) in dimethylformamide (6 mL). The mixture was heated to 50°C, and a solution containing methanesulfonyl chloride (1 mL) in dry dimethylformamide (1.5 mL) was slowly added. Subsequently, the mixture was heated to 80°C

for 1 h, then cooled to room temperature and placed into a large volume of ice-cold sodium acetate aqueous solution (1.46 M). The mixture was then extracted with ethyl acetate, and the organic layer was dried and concentrated. The residue was recrystallized from ethanol to obtain 734THI (0.34 g, 63%). The purity of 734THI, as determined by high-performance liquid chromatography (HPLC) analysis, was higher than 95%. Electrospray ionization- mass spectrometry (ESI-MS) $[M+H]^+$: 270.81 g/mol. ^{1}H nuclear magnetic resonance (NMR) (200 MHz, DMSO-d_6) δ: 6.78–6.80 (1H, m, 5′-H), 6.85 (1H, d, *J*=2.2 Hz, 6′-H), 6.90 (1H, d, *J*=2.4 Hz, 8-H), 6.95 (1H, d, *J*=2.2 Hz, 6-H), 7.02 (1H, d, *J*=1.4 Hz, 2′-H), 7.96 (1H, d, *J*=8.6 Hz, 5-H), 8.24 (1H, s, 2-H), 8.95 (1H, s, 3′-OH), 8.98 (1H, s, 4′-OH), 10.78 (1H, s, 7-OH).

Phase solubility studies

Phase solubility studies were performed in compliance with the method of Higuchi and Connors.[24] In brief, an excess amount of raw 734THI was added to 1 mL of pure water containing different concentrations of PVP K30 (ranging from 1 to 27 mg). The suspensions were vigorously shaken for 24 h at room temperature using a vibrator (Vortex-Gene 2, Scientific Industries, Inc., NY, USA), and then the solution was filtered through a 0.45 μm syringe filter (13 mm Acrodisc® syringe filters with GHP membrane; Pall Corporation, NY, USA). The concentration of 734THI in each sample was analyzed by the HPLC method. The stability constants (Ks) were calculated according to the slope of the straight portion of the phase solubility diagram. Equation 1 is as follows:

$$Ks = \frac{Slope}{S_0\ (1 - slope)} \quad (1)$$

where S_0 is the 734THI solubility in pure water.

Preparation of 734THI nanoparticle powder (734THIN) by planetary ball mill technique

In a binary system, 734THI was mixed with PVP K30 at a weight ratio of 1:19. The mixture was placed in a 250 mL milling agate jar with 10 agate balls of 20 mm and then grinded by planetary ball mill (PM 100; Retsch GmbH & Co., Haan, Germany). The operating parameters were set at 400 rpm for 30 min at room temperature. Subsequently, the 734THIN was collected and stored at room temperature until further analysis. In addition, 734THI–PVP physical mixture was prepared by mixing in glass vials using a vortex mixer for 3 min.

Standard curve of 734THI obtained by HPLC analysis

The chromatographic system was composed of an L-2130 pump, L-2200 autosampler and L-2420 ultraviolet (UV)–vis detector. The retention time and concentration of 734THI were evaluated using the Mightysil RP-18 GP column (250×4.6 mm, internal diameter, 5 μm; Kanto Corporation, Portland, OR, USA). The mobile phase was a mixture of 10 mM phosphate buffer and acetonitrile (65:35) and its pH was adjusted to 2.9 with phosphoric acid. The flow rate was set at 1 mL/min, and the wavelength of UV detector was kept at 262 nm. The calibration curve of 734THI was linear (r^2>0.99) within the range 0.05–50 μg/mL.

Morphology and particle size analysis

The particle size and polydispersity index of raw 734THI and its nanoparticle powder were analyzed using a particle analyzer with dynamic light scattering technique (Malvern Zetasizer 3000 HS analyzer inspection system; Malvern Instruments Ltd, Malvern, UK) at 25°C and an angle of 90°. The samples were diluted with pure water. Each value was measured in triplicate. In addition, the morphology and size of raw 734THI and 734THIN were visualized under SEM (Hitachi S4700; Hitachi, Tokyo, Japan) and TEM (JEM-2000EXII instrument; JEOL Co., Tokyo, Japan).

Yield and drug loading

For determining the yield of 734THIN, 734THIN was accurately weighed and dissolved in methanol in a 1.5 mL microtube. The 734THI concentration of the sample was determined by the reversed-phase HPLC method as described above.

The yield (%) of 734THIN was calculated using Equation 2:

$$\text{Yield (\%)} = \frac{\text{Total weight of 734THIN}}{\text{Total weight of 734THI and PVP}} \times 100\% \quad (2)$$

The drug loading of 734THIN was determined using the ultrafilter (molecular weight 10,000 Da) to separate loaded and unloaded 734THI. Equivalent amount of 1 mg 734THI from 734THIN was accurately weighed and dissolved in 1 mL pure water and immediately centrifuged at 10,000 rpm for 30 min. The drug loading of 734THI from the nanoparticle powder can be calculated using Equation 3:

$$\text{Drug loading (\%)} = \frac{\text{Total 734THI} - \text{Unloading 734THI of 734THIN}}{\text{Total 734THI content of 734THIN}} \times 100\% \quad (3)$$

FT-IR spectroscopy

About 2–3 mg of each sample was mixed with potassium bromide and grounded well using an agate mortar. The powder was compressed into a disk (12 mm) at 10 ton pressure. The FT-IR spectrum of each sample was obtained using the Perkin-Elmer 2000 spectrophotometer (Perkin-Elmer, Norwalk, CT, USA) over the range of 400–4,000 cm^{-1} to determine the molecular states of all samples. Analysis of the spectrum was performed by the spectrum V2.00 software.

Powder X-ray diffractometry

The crystalline form of 734THI and its nanoparticle powder was analyzed by XRD with a Siemens D5000 diffractometer (Siemens, Munich, Germany) under the following conditions: Cuk_{α} radiation at 40 kV and current of 40 mA. The instrument was operated in a continuous scan mode over a range of 2θ angles (5°–50°) with the scanning rate at 1°/min.

^{1}H NMR measurement

The ^{1}H NMR patterns of 734THI and 734THIN were analyzed using a Varian Mercury Plus AS400 NMR System (Oxford Instrument Co., Abingdon, UK). To analyze the ^{1}H NMR spectra, samples containing 5 mg 734THI were dissolved in 0.5 mL of DMSO-*d*6 in an ^{1}H NMR tube and recorded by an ^{1}H NMR instrument. Chemical shifts were referenced in parts per million (ppm).

Aqueous solubility of 734THI and 734THIN

Each sample containing 1 mg 734THI was added to 1 mL of pure water in a 1.5 mL microtube and stirred with a shaker at 1,000 rpm for 10 min. After that, the samples were filtered using a syringe filter (0.45 μm). The concentration of 734THI in each sample was analyzed by HPLC as described above.

Cell viability of 734THIN-treated HaCaT keratinocytes

HaCaT keratinocytes were cultured in DMEM containing 10% fetal bovine serum, 100 units/mL penicillin G, 100 μg/mL streptomycin and 0.25 μg/mL amphotericin B. Cells were maintained in a 37°C incubator with 5% CO_2. Then 1×10^4 HaCaT keratinocytes were seeded in each well in 96-well culture plates. After 24 h incubation, various concentrations of 734THIN were added into each well for 24 h. After treatment, the medium was removed, wells were washed with PBS twice and 150 μL of MTT solution (0.5%, w/v) was added into each well. The plate was placed in an incubator at 37°C. After that, the MTT solution was removed and 100 μL of DMSO was added into each well. The absorbance of each well was measured at 550 nm using a microplate spectrophotometer (μQuant; Biotek Instruments Inc., Winooski, VT, USA). The absorbance of HaCaT cells treated with PBS was used as the control for calculating the cell viability. All measurements were performed in triplicate.

Cellular uptake in HaCaT keratinocytes

HaCaT keratinocytes were seeded at a density of 2×10^5 cells/well in a 12-well plate and incubated for 24 h. HaCaT keratinocytes were treated with 80 μg/mL of raw 734THI, its physical mixture (734THI–PVP PM) or 734THIN for 2 h. After treatment, the culture medium was collected and the cells were washed with PBS twice and lysed with 0.2% sodium dodecyl sulfate followed by extraction with methanol under sonication for 30 min in a sonicator bath. All samples were then filtered through a 0.45 μm syringe filter and the concentration of 734THI was determined by the HPLC method as described above.

Determination of PM-induced HaCaT keratinocyte injury

The PM-induced HaCaT keratinocytes model was built as described previously.[25] Briefly, PM was suspended in PBS and then sonicated for 30 min in a sonicator bath. HaCaT keratinocytes (1×10^6 cells per well in a six-well plate) were treated with raw 734THI in PBS or 734THIN in PBS for 1 h. After that, 50 μg/cm^2 of PM was added into each well for different periods of time. Experiments were undertaken within 1 h of PM preparation to prevent variations in PM composition. The cells were then washed with PBS twice and total proteins were lysed with lysis buffer (20 mM Tris-HCl, 150 mM NaCl, 1 mM EDTA, 1 mM ethylene glycol tetraacetic acid, 1% Triton X-100, 1 mM phenylmethylsulfonyl fluoride, pH 7.4). For Western blotting assay, sodium dodecyl sulfate-polyacrylamide gel electrophoresis was performed using a 10% running gel, and then the proteins were transferred onto poly(vinylidene fluoride membranes. The membranes were incubated with primary antibodies, including COX-2 (1:1,000), cPLA2 (1:1,000), ICAM (1:1,000), MMP-9 (1:1,000), GAPDH (1:5,000), phospho-ERK (1:1,000), phospho-p38 (1:1,000) and phospho-JNK (1:1,000), overnight at 4°C, washed with Tris-buffered saline with Tween-20, incubated with anti-mouse or anti-rabbit HRP-conjugated secondary antibodies for 1 h at room temperature, and then washed with Tris-buffered saline with Tween-20 again. Immunoreactive bands of each sample were reacted with enhanced chemiluminescence reagents and visualized using the Alphatec system.

Statistical analysis

All data were analyzed by Microsoft Excel 2010 software (Microsoft Office, Microsoft Corporation, WA, USA) and

expressed as mean ± SD. Significant difference of all data was analyzed using one-way analysis of variance with Tukey's post hoc test by SPSS software version 14 (SPSS Inc., Chicago, IL, USA). *P*-value <0.05 was considered statistically significant.

Results

Particle size and morphology of 734THIN

As shown in Table 1, the particle sizes of raw 734THI and 734THIN were 4,849.0±256.9 and 392.6±5.1 nm, respectively, and the polydispersity index values were >1 and 0.43±0.13, respectively. We also observed the morphology of raw 734THI and its nanoparticle powder (734THIN) under SEM. Figure 1A shows that raw 734THI had irregular thick slice morphology and its length was over 50 μm, whereas 734THIN displayed small and irregular round particles and its size was <20 μm (Figure 1B). In addition, 734THIN was resuspended in water and then observed by TEM. Figure 1C shows that the particle morphology of 734THIN displayed small spherical shapes and its particle size was <400 nm. Moreover, the yield and the drug loading capacity of 734THIN were 81.7% and 65%, respectively. These results suggest that PVP K30 is an effective polymer to prepare the 734THIN formulation.

Solubility of raw 734THI and 734THIN

It is well known that hydrophilic polymers such as PVP and polyvinyl alcohol can be used to increase the aqueous solubility and bioavailability of BCS II and IV compounds.[11,26] PVP K30 is a nontoxic agent in oral formulations and also a non-irritating and non-sensitizing agent in topical formulations. Therefore, the present study used PVP K30 as an excipient to prepare 734THIN by planetary BMT. Phase solubility analysis is usually performed to confirm the usage of excipient before preparing pharmaceutical formulations.[24,27] The data from the phase solubility experiment indicated that PVP K30 effectively increased the solubility of 734THI in a concentration-dependent manner. The phase solubility diagram of 734THI with PVP K30 showed an A_L-type (A_L type means the solubility of 734THI increases with increasing PVP concentration) relationship which indicated that the complex of 734THI–PVP K30 is of first order with respect to excipient (Figure 1D). In addition, the Ks value of 734THI with PVP K30 is 272.7 mM^{-1}, indicating the spontaneous nature of strong stability. According to these results, the ratio 734THI:PVP K30 (1:19) was used in the co-grinding method. In addition, the Noyes–Whitney equation indicates that enhancement of drug solubility can effectively improve the dissolution rate of the raw drug. Our data showed that the aqueous solubility of raw 734THI and 734THIN was 20.21±0.13 and 792.81±0.31 μg/mL, respectively, indicating that the solubility of 734THIN was effectively increased 40-fold compared to raw 734THI.

Table 1 Particle size and polydispersity index, yield, drug loading and aqueous solubility of 734THI nanoparticle powder

	Particle size (nm)	Polydispersity index	Yield (%)	Drug loading (%)	Aqueous solubility (μg/mL)
734THI	4,849±256.9	>1	–	–	20.21±0.13
734THIN	392.6±5.1*	0.437±0.13	81.67	65	792.81±0.31*

Note: *Significantly different from 734THI (*P*<0.05).
Abbreviations: 734THI, 7,3′,4′-trihydroxyisoflavone; 734THIN, 734THI nanoparticle powder.

Amorphous transformation of 734THIN

In this study, we used powder XRD to evaluate the crystalline to amorphous transformation of raw 734THI and 734THIN. As seen in Figure 2, several obvious diffraction peaks are displayed in the XRD pattern of raw 734THI, occurring at 9.1°, 22.6°, 23.6°, 27.9° and 36.7°, which indicates that 734THI has a crystalline structure. After co-grinding of 734THI, the characteristic peaks in the XRD pattern of 734THIN were reduced. These results indicated that 734THI grinded with PVP K30 can transform the crystalline structure of 734THI to an amorphous state.

Hydrogen bond formation

^{1}H NMR and FT-IR are usually used to confirm the hydrogen bonding interactions between a drug and an excipient. In the ^{1}H NMR spectrum of raw 734THI, the resonance peaks for aromatic protons and phenolic protons occurred at δ6.7–8.3 and δ8.9–10.8, respectively. There were three obvious signals for phenolic protons on 734THI, occurring at δ10.798 (C7–OH), δ9.029 (C4′–OH) and δ8.981 (C3′–OH), but these signals were not found in the ^{1}H NMR spectrum of 734THIN (Figure 3A). These findings demonstrated that the phenolic–OH on the A and B rings of raw 734THI may interact with PVP K30 after co-grinding preparation, and then form intermolecular hydrogen bonds which may contribute to the improved aqueous solubility of raw 734THI. In addition, the FT-IR patterns of raw 734THI and 734THIN are shown in Figure 3B. The FT-IR spectrum of 734THI showed several characteristic peaks, including a broad band at 3,420–3,100 cm^{-1} (phenolic–OH), 1,600–1,400 cm^{-1} (aromatic C=C stretching), 1,626 cm^{-1} (C=O, stretching vibration) and 1,288 cm^{-1} (C–O–H stretching). After co-grinding, the FT-IR spectrum of 734THIN showed that the phenolic–OH stretch of 734THI became broadened and completely disappeared at 3,422 cm^{-1}. These results demonstrated that hydrogen bonds were formed between the

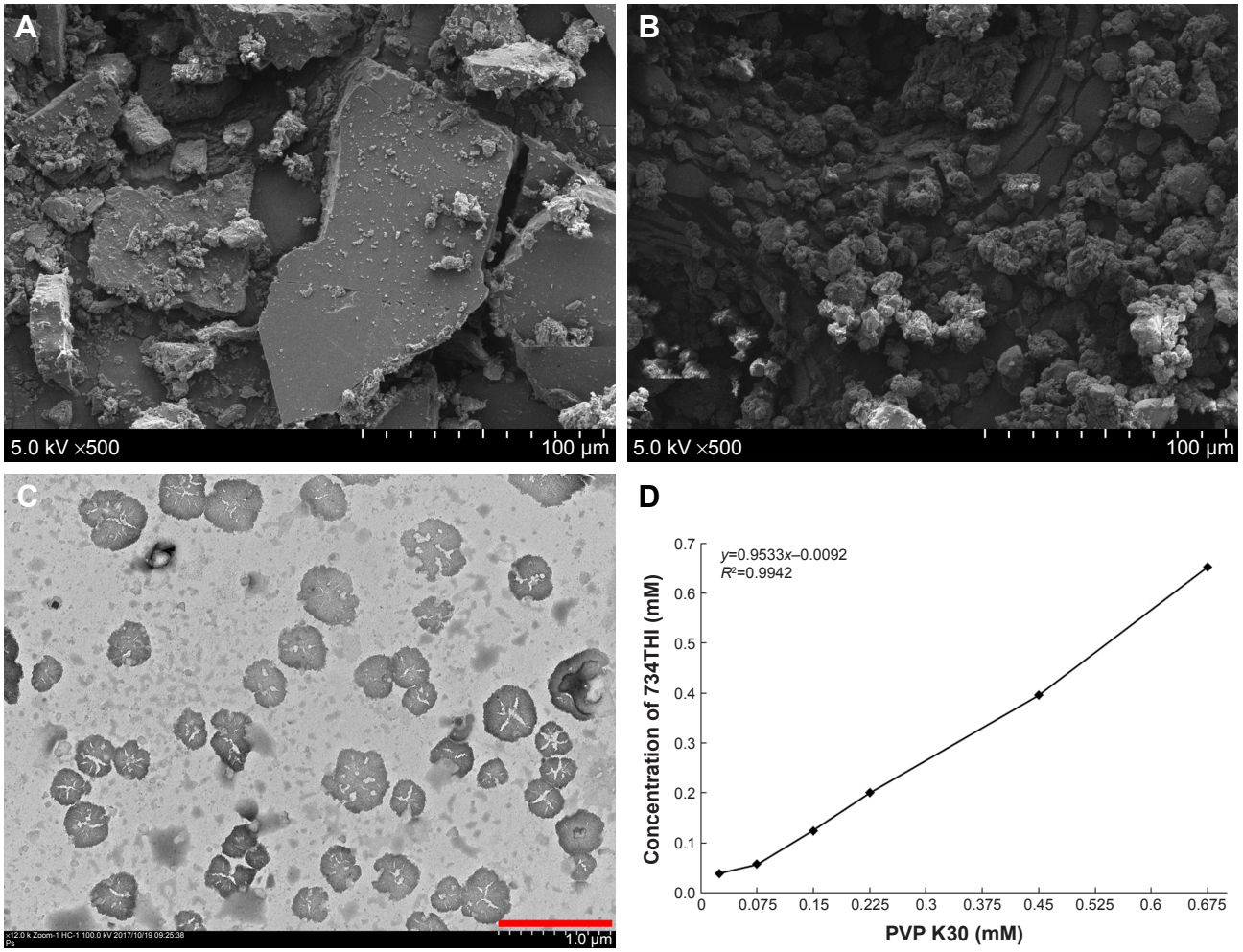

Figure 1 The scanning electron microscopy photographs of raw 734THI (**A**) and 734THIN (**B**), the transmission electron microscopy photograph of 734THIN (**C**, scale bar=1 µm) and the phase solubility diagram of 734THI with PVP K30 (**D**).
Abbreviations: 734THI, 7,3′,4′-trihydroxyisoflavone; 734THIN, 734THI nanoparticle powder; PVP K30, polyvinylpyrrolidone.

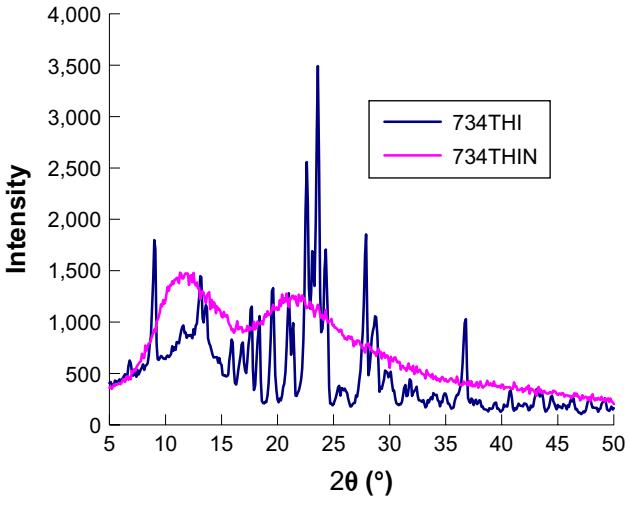

Figure 2 Crystalline form of raw 734THI and 734THIN using powder XRD analysis.
Abbreviations: 734THI, 7,3′,4′-trihydroxyisoflavone; 734THIN, 734THI nanoparticle powder; XRD, powder X-ray diffractometry.

hydroxyl groups of 734THI and PVP K30 after the planetary ball mill co-grinding process.

Cell viability and cellular uptake of 734THIN

It is very important that a good pharmaceutical formulation not only shows effective pharmacologic activity but also has low cytotoxicity. In the present study, we treated HaCaT keratinocytes with 5, 10, 20, 40 and 80 µM of 734THIN and determined cell viability by the MTT assay. As seen in Figure 4A, 734THIN concentrations ranging from 5 to 80 µM did not show obvious cytotoxicity after 24 h of treatment. Under microscopic observation, the cell morphologies following 734THIN treatment did not show cytotoxic patterns such as cell vacuolization, detachment, lysis or changes in membrane integrity (data not shown). These findings indicated that 734THIN is a non-cytotoxic formulation and it can be applied in medicine and as a cosmetic product. For cellular uptake, HaCaT

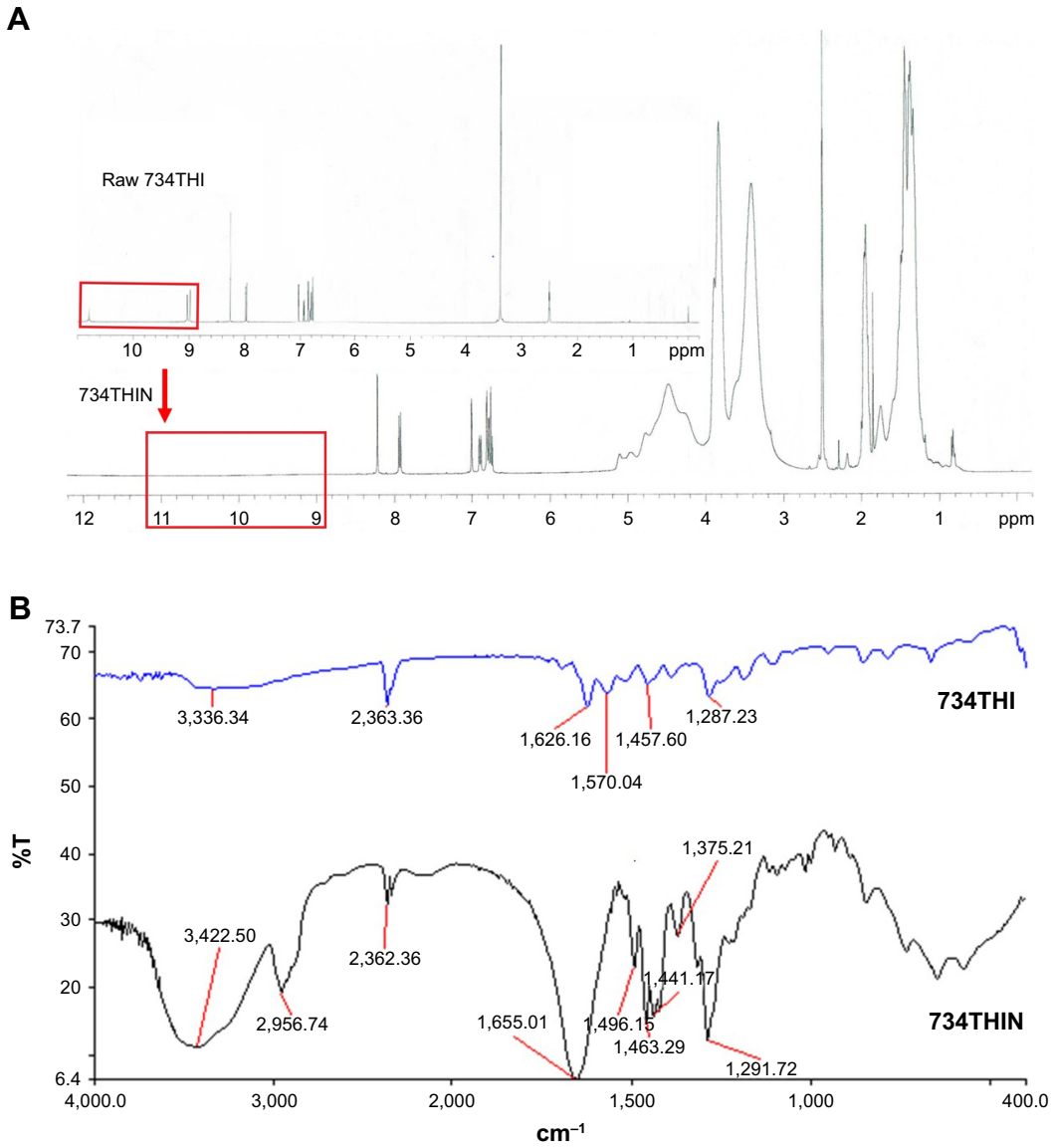

Figure 3 Hydrogen bonding interactions between 734THI and PVP K30. ^{1}H NMR (**A**) and FT-IR (**B**).
Abbreviations: 734THI, 7,3′,4′-trihydroxyisoflavone; 734THIN, 734THI nanoparticle powder; FT-IR, Fourier transformation infrared spectroscopy; PVP K30, polyvinylpyrrolidone.

keratinocytes treated with 734THIN (227.92±23.70 nM) displayed greater cellular absorption in the intracellular compartment than raw 734THI (48.86±6.11 nM) or its physical mixture (128.06±12.34 nM), as shown in Figure 4B. These results indicated that 734THIN enhanced the penetration of 734THI into HaCaT keratinocytes due to particle size reduction.

Anti-pollutant activity of 734THIN in PM-induced HaCaT keratinocytes

As shown in Figure 5, exposure of HaCaT keratinocytes to PM at 50 μg/cm^2 significantly increased the expression of COX-2, cPLA2 and ICAM, when compared to the non-exposed group. Pretreatment of PM-exposed HaCaT keratinocytes with raw 734THI in DMSO or 734THIN in PBS inhibited the expression of these inflammatory proteins in a dose-dependent manner; however, pretreatment with raw 734THI in PBS had no significant inhibitory effect. The present study also demonstrated that treatment of HaCaT keratinocytes with PM at 50 μg/cm^2 resulted in overexpression of MMP-9 protein, when compared to the non–PM-exposed group. Pretreatment of PM-exposed HaCaT keratinocytes with raw 734THI in DMSO or 734THIN in PBS significantly decreased MMP-9 expression in a dose-dependent manner, but 734THI in PBS did not show any inhibitory effect. These results indicated that 734THIN may exhibit antiaging activity in PM-exposed HaCaT keratinocytes by reducing MMP-9 expression. Figure 6 shows that treatment of HaCaT keratinocytes with

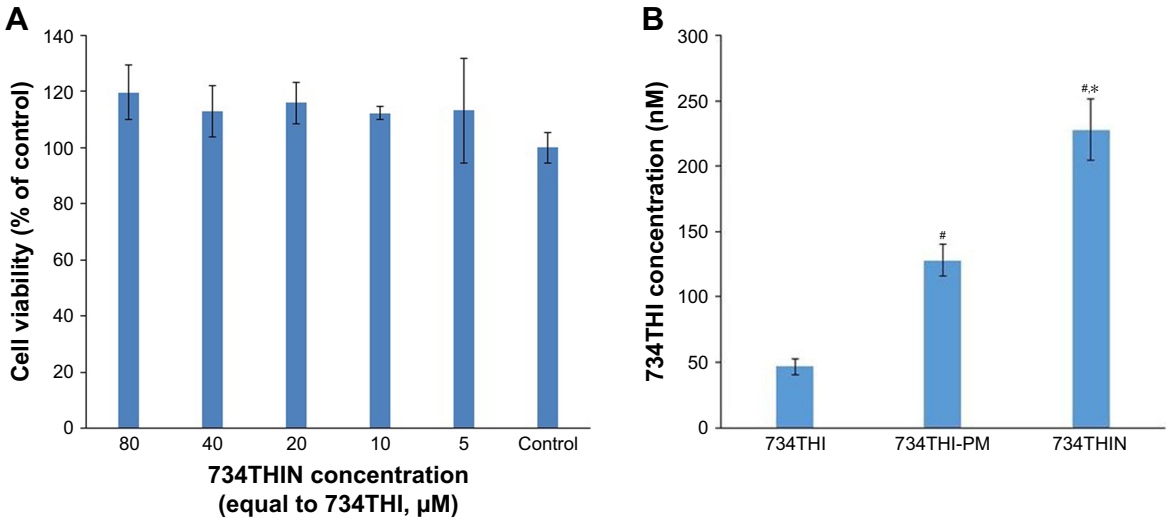

Figure 4 Cell viability of HaCaT keratinocytes treated with 734THIN for 24 h (**A**) and cellular uptake of 734THIN by HaCaT keratinocytes after 2 h (**B**).
Notes: The different superscript symbols indicate significant differences. #Significantly different from raw 734THI ($P<0.05$). *Significantly different from 734THI-PM ($P<0.05$). The experiments were performed in triplicate.
Abbreviations: 734THI, 7,3′,4′-trihydroxyisoflavone; 734THIN, 734THI nanoparticle powder; 734THI-PM, 734THI physical mixture.

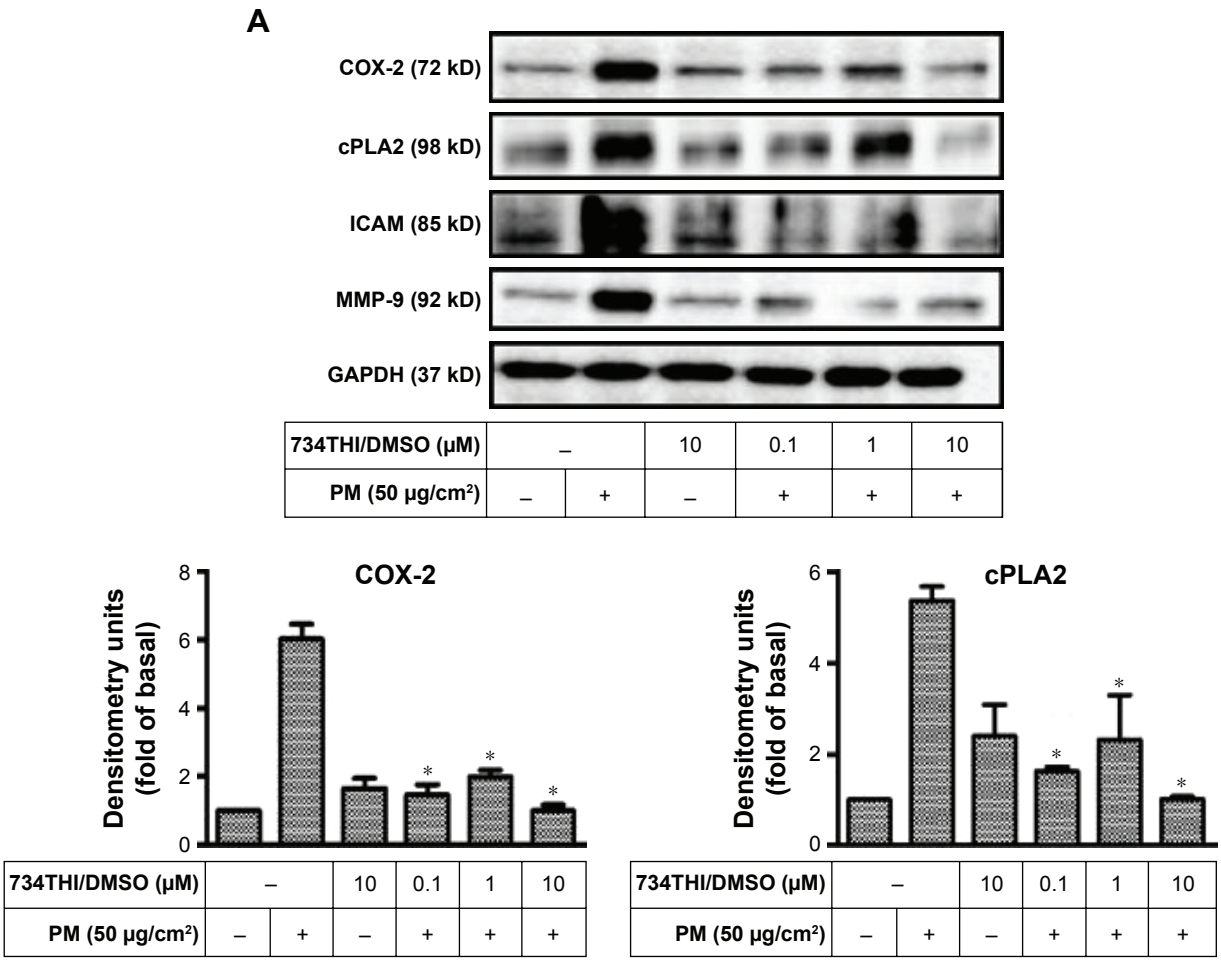

Figure 5 (*Continued*)

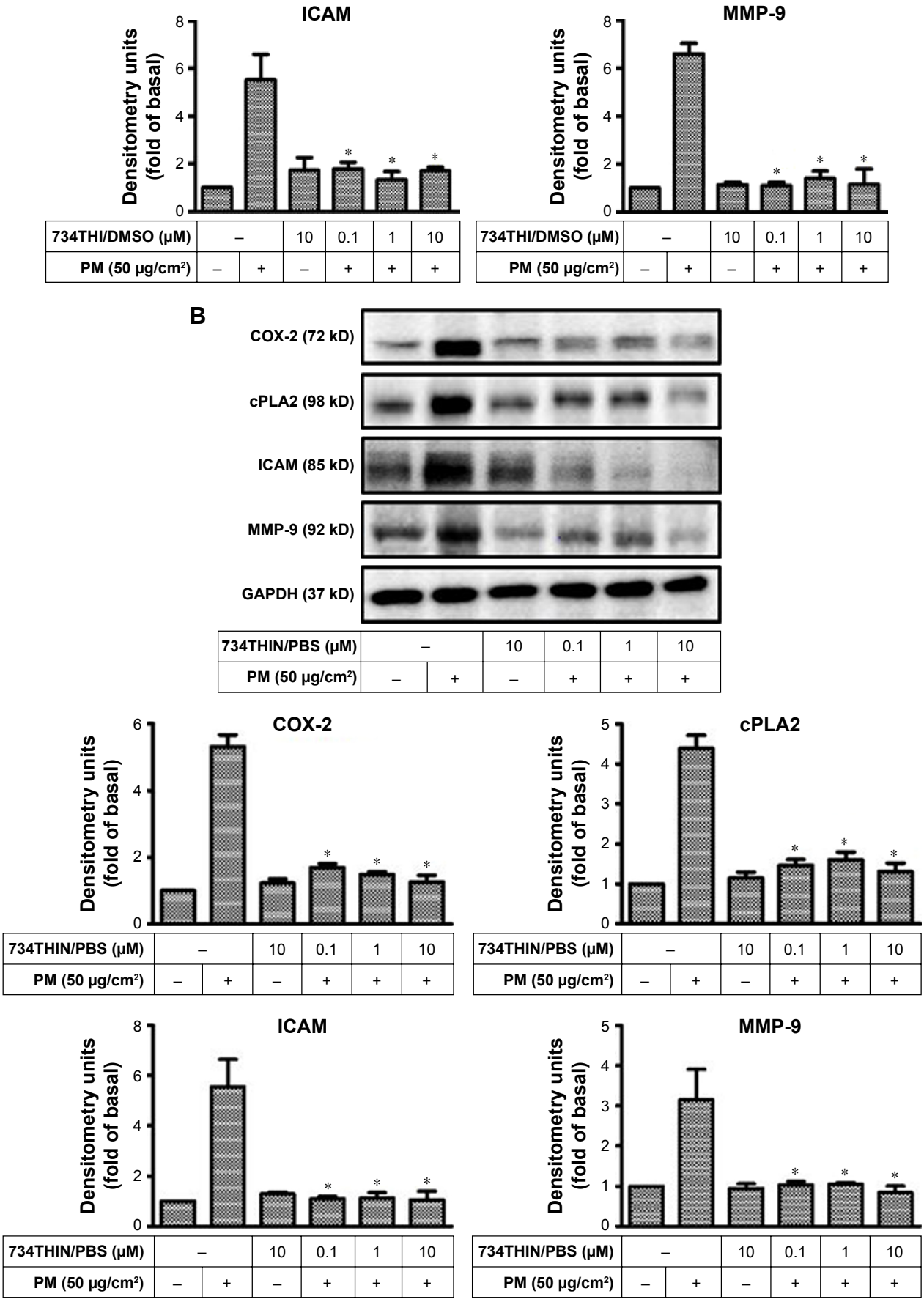

Figure 5 (*Continued*)

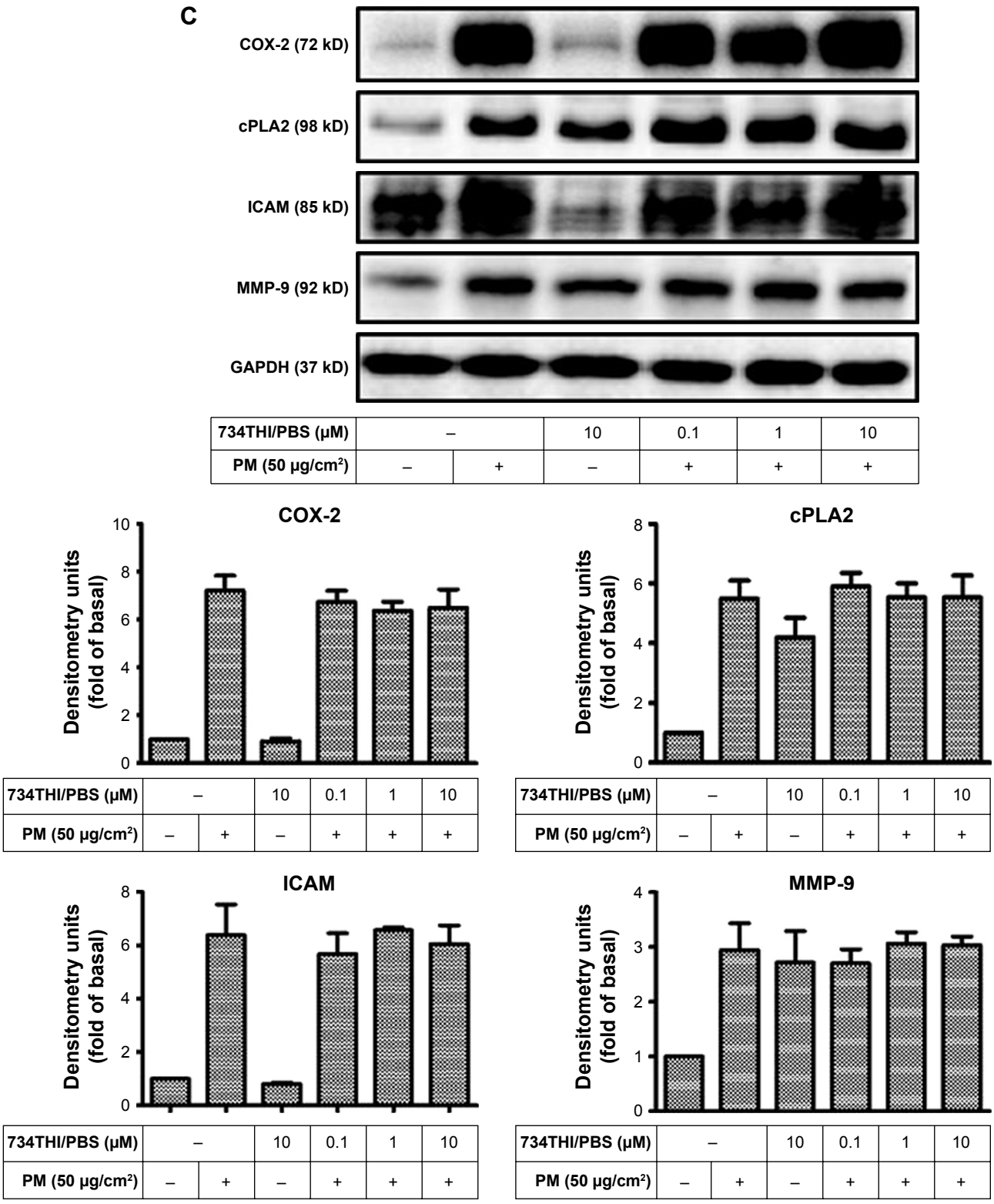

Figure 5 Expression of inflammatory proteins (COX-2, cPLA2, ICAM) and aging protein (MMP-9) following various 734THI treatments in PM-exposed HaCaT keratinocytes: 734THI in 1% DMSO (**A**), 734THIN in PBS (**B**) and raw 734THI in PBS (**C**).

Notes: *Significantly different from PM-induced only group ($P<0.05$). The experiments were performed in triplicate.

Abbreviations: 734THI, 7,3′,4′-trihydroxyisoflavone; 734THIN, 734THI nanoparticle powder; DMSO, dimethyl sulfoxide; ICAM, intercellular adhesion molecule 1; PBS, phosphate buffered saline; PM, particulate matter; PVP, polyvinylpyrrolidone.

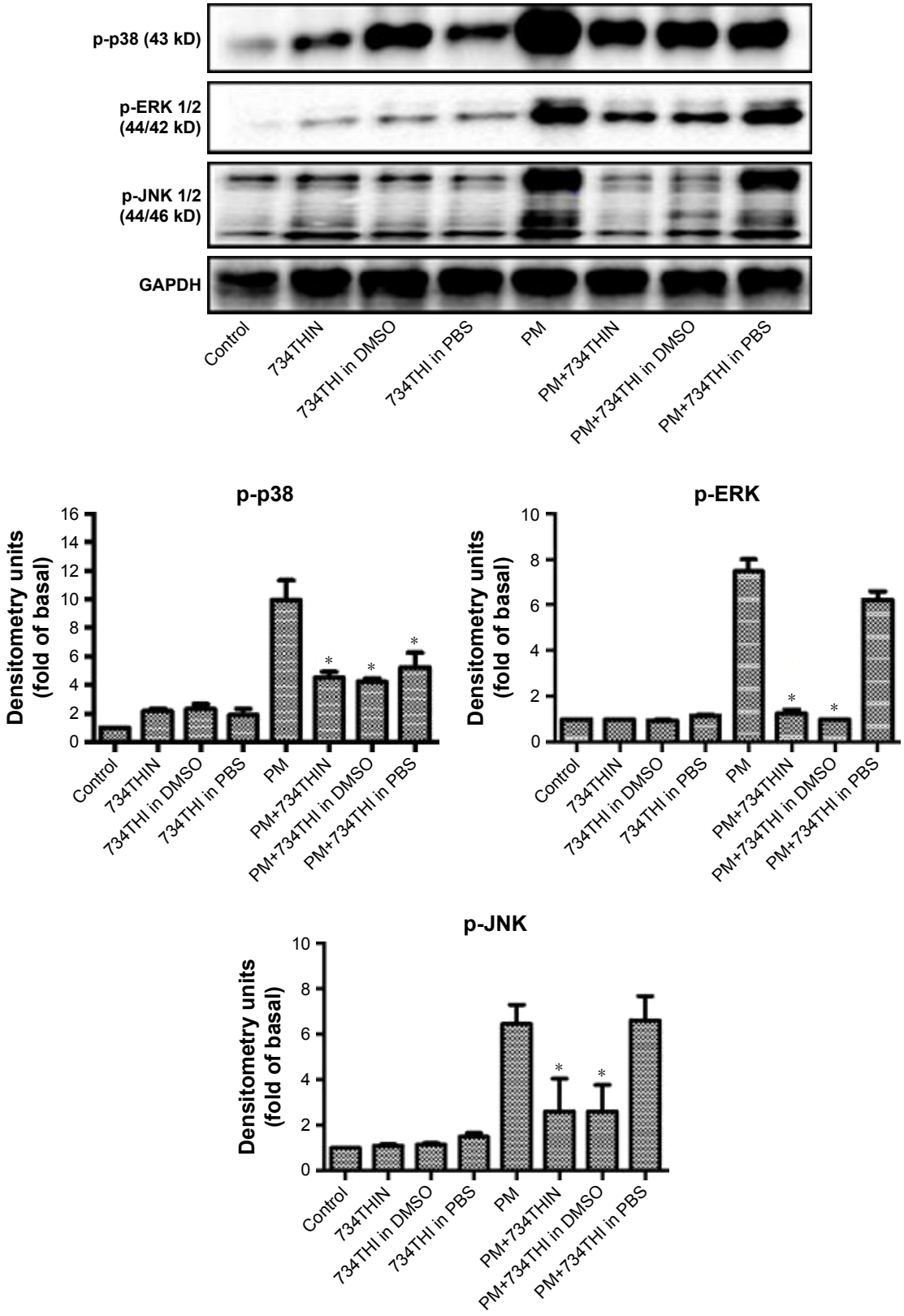

Figure 6 Expression of MAPK signaling proteins (p-p38, p-ERK 1/2, p-JNK 1/2) following various 734THI treatments at 10 μM in PM-exposed HaCaT keratinocytes.
Notes: *Significantly different from PM-induced only group ($P<0.05$). The experiments were performed in triplicate.
Abbreviations: 734THI, 7,3′,4′-trihydroxyisoflavone; 734THIN, 734THI nanoparticle powder; DMSO, dimethyl sulfoxide; PBS, phosphate buffered saline; PM, particulate matter.

PM induced the phosphorylation of mitogen-activated protein kinases (MAPKs) including ERK, p38 and JNK, when compared to the non–PM-exposed group. Pretreatment of PM-exposed HaCaT keratinocytes with 734THIN in PBS suppressed the phosphorylation of ERK, p38 and JNK. These results indicate that 734THIN could inhibit the phosphorylation of ERK, p38 and JNK, which are responsible for the overexpression of COX-2 and MMP-9. Therefore, 734THIN maintained its anti-pollutant activity after planetary ball mill co-grinding preparation process.

Discussion

Based on our knowledge, many drugs have useful biological activities, but their poor aqueous solubility leads to insufficient concentration and subsequently results in poor bioavailability. Colombo et al reported that co-grinding is an effective method to induce mechanochemical activation of drugs and improve the aqueous solubility and bioavailability of drugs. This may be achieved by particle size reduction, transformation from crystalline state to amorphous state and enhancement of molecular interactions.[28] Regarding particle size reduction, the increase in surface area of drugs is a promising way to improve their aqueous solubility. Salazar et al indicated that reduction of particle size into the nanometer range can increase the surface area of drugs to improve their aqueous solubility and bioavailability.[29] Our results demonstrated that 734THI co-grinded with PVP K30 can reduce the particle size about 12-fold, and increase the aqueous solubility about 39-fold, when compared to raw 73THI. These results indicated that 734THI complexed with PVP K30 after planetary ball mill preparation has smaller particle size and more uniform particle size distribution, when compared to raw 734THI. A possible explanation for this result is that PVP K30 may act as a hydrophilic polymer vehicle for dispersing and suspending compounds with poor aqueous solubility, as has been shown for chlorzoxazone,[30] clarithromycin[31] and dipfluzine.[32] Previous studies have indicated that PVP K30 serves as a good solubilizing agent to overcome the poor aqueous solubility of drugs such as curcumin[33] and silymarin.[34] Our results also demonstrated that PVP K30 is an appropriate excipient to reduce the particle size and increase the aqueous solubility of raw 734THI using planetary BMT. Moreover, Khutoryanskiy reported that polymers formulated with poorly soluble drugs may improve their aqueous solubility by forming intra- and intermolecular hydrogen bonds.[35] Our data demonstrated that PVP K30 can interact with the phenolic–OH of raw 734THI to form a hydrogen-bonded interpolymer complex and improve its aqueous solubility. These findings indicated that 734THIN can improve the aqueous solubility of 734THI through increasing the surface area of raw 734THI and formation of hydrogen bonds between PVP K30 and 734THI. The related schematic diagram for the chemical structure of 734THIN is presented in Figure 7.

Drugs with poor aqueous solubility possess several physicochemical properties, such as crystalline structure, lower free energy, melting event, birefringence and ordered state,

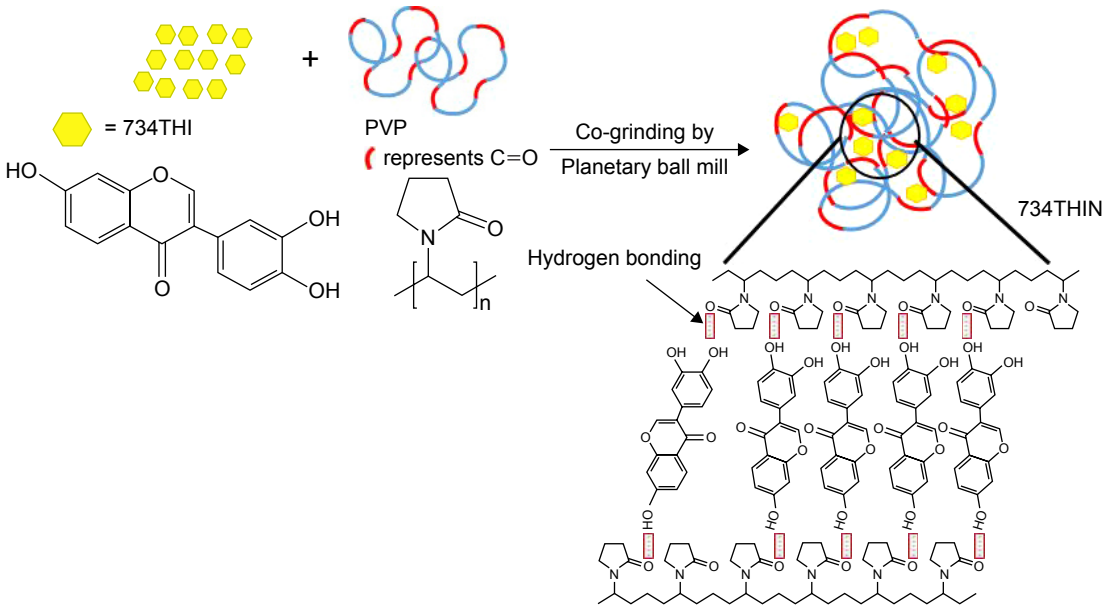

Figure 7 The related schematic diagram for the chemical structure of 734THIN.
Abbreviations: 734THI, 7,3′,4′-trihydroxyisoflavone; 734THIN, 734THI nanoparticle powder; PVP, polyvinylpyrrolidone.

which may limit their aqueous solubility and lead to poor dissolution and bioavailability. Amorphous nanoparticles, also called nanosized amorphous formulations, have been utilized to increase the solubility of poorly soluble drugs through improving their physicochemical properties, including halo pattern, free energy enhancement, glass transition event, absence of birefringence and disordered state.[36] Co-grinding technique, one of the methods for manufacturing amorphous nanoparticles, is commonly used to transform the crystalline structure of the active ingredient drug into an amorphous form to increase its aqueous solubility and has been used for drugs such as fenofibrate, griseofulvin and sirolimus.[36] Our results demonstrated that 734THI co-grinded with PVP K30 effectively transformed the crystalline state of raw 734THI to amorphous nanoparticles (Figure 2). Jain and Banga have demonstrated that PVP acts as a crystallization inhibitor and can increase the amorphous transformation of drugs with poor aqueous solubility by forming disordered structures with higher free energy, which can then improve their aqueous solubility, dissolution rate and bioavailability.[37]

Kim et al reviewed the detrimental effects of airborne PM in various skin diseases and mentioned that PM is a damaging component of air pollution, which can cause both direct and indirect damage to the skin barrier.[38] Exposure to PM may result in the activation of a number of signaling pathways involved in pathophysiological processes, leading to inflammatory skin conditions such as atopic dermatitis, acne, alopecia, skin cancer and aging. PM overexposure may induce overexpression of the proinflammatory protein cyclooxygenase 2, a rate-limiting factor involved in the overproduction of prostaglandin E2, which can then promote skin inflammation. Moreover, PM, including urban fine particles[39] and cigarette smoking,[40] has been shown to be a major factor involved in extrinsic aging, leading to skin thickening and wrinkle formation. It is well known that chronic exposure to PM[39] and ultraviolet light[41] may lead to elevated expression of matrix metalloproteinases, which can degrade the collagen fibrils and extracellular matrix produced by epidermal keratinocytes and dermal fibroblasts. MMP-9 is a well-known gelatinase and type IV collagenase, which is overexpressed by HaCaT keratinocytes when the cells are overexposed to PM or UVB, resulting in skin aging by collagen degradation. In addition, overexposure of cells to UVB or PM can trigger the activation of MAPKs, including ERK, JNK and p38 kinase, which may induce the overexpression of COX-2 and MMP-9 and lead to the development of skin inflammation and aging.[41] Previous studies have demonstrated that many natural compounds, such as curcumin[42] and resveratrol,[43] can effectively downregulate the phosphorylation of MAPKs and contribute to the activation of nuclear transcription factors such as c-Fos and NF-κB in pollutant-exposed cells. In addition, Loh et al reported that amorphous drug formulations are unstable and may reduce the biological activities of the drug;[44] therefore, the present study sought to confirm the anti-pollutant activity of 734THIN in PM-exposed HaCaT keratinocytes. Our results revealed that 734THIN can inhibit the expression of COX-2 and MMP-9 induced by PM treatment through downregulating the phosphorylation of ERK, JNK and p38. In addition, the results in Figure 6 show that 734THI in DMSO and 734THIN in PBS significantly downregulated the phosphorylation of ERK and JNK, when compared to 734THI in PBS, but there was no significant difference in the phosphorylation of p38. A possible explanation is that for 734THI in DMSO and 734THIN in PBS, enough concentration of 734THI may have been absorbed by HaCaT keratinocytes to downregulate the phosphorylation of ERK and JNK, but this concentration may not be sufficient to effectively inhibit the phosphorylation of p38. The anti-inflammatory and antiaging activities of 734THIN were similar to those of raw 734THI in DMSO solution, and 734THIN also displayed greater biological activities than raw 734THI in water due to higher 734THI content in HaCaT keratinocytes. According to these findings, 734THI co-grinded with PVP K30 maintained its anti-pollutant activity in PM-exposed HaCaT keratinocytes, and therefore, 734THIN is a stable amorphous nanoparticle formulation.

In conclusion, the results from the present study revealed that 734THI after co-grinding by planetary ball mill preparation showed increased aqueous solubility and cellular uptake by improvement in physicochemical properties, including particle size reduction, crystalline to amorphous transformation and intermolecular hydrogen bonding with PVP K30. We also demonstrated that 734THIN in PBS can inhibit the overexpression of COX-2 and MMP-9 through downregulating MAPK pathway signaling in PM-exposed HaCaT keratinocytes, whereas raw 734THI in PBS with low aqueous solubility did not show any anti-inflammatory or antiaging activity. Therefore, 734THIN may be used as an additive in anti-pollutant skin care products for preventing PM-induced skin inflammation and aging.

Acknowledgments

This work was supported by grants from the Ministry of Science and Technology, Taipei, Taiwan, Republic of China (MOST 104-2320-B-037-009) and Kaohsiung Medical University Research Foundation (KMU-M106030).

Disclosure

The authors report no conflicts of interest in this work.

References

1. Puri P, Nandar SK, Kathuria S, Ramesh V. Effects of air pollution on the skin: a review. *Indian J Dermatol Venereol Leprol*. 2017;83(4):415–423.
2. Bekki K, Ito T, Yoshida Y, et al. PM2.5 collected in China causes inflammatory and oxidative stress responses in macrophages through the multiple pathways. *Environ Toxicol Pharmacol*. 2016;45:362–369.
3. Gong P, Chen F, Liu X, Gong X, Wang J, Ma Y. Protective effect of caffeic acid phenethyl ester against cadmium-induced renal damage in mice. *J Toxicol Sci*. 2012;37(2):415–425.
4. Huerta-García E, Montiél-Dávalos A, Alfaro-Moreno E, Gutiérrez-Iglesias G, López-Marure R. Dehydroepiandrosterone protects endothelial cells against inflammatory events induced by urban particulate matter and titanium dioxide nanoparticles. *Biomed Res Int*. 2013;2013:382058.
5. Sticozzi C, Cervellati F, Muresan XM, Cervellati C, Valacchi G. Resveratrol prevents cigarette smoke-induced keratinocytes damage. *Food Funct*. 2014;5(9):2348–2356.
6. Franke AA, Custer LJ, Cerna CM, Narala KK. Quantitation of phytoestrogens in legumes by HPLC. *J Agric Food Chem*. 1994;42:1905–1913.
7. Kim BB, Kim JR, Kim JH, et al. 7,3′,4′-trihydroxyisoflavone ameliorates the development of dermatophagoides farinae-induced atopic dermatitis in NC/Nga mice. *Evid Based Complement Alternat Med*. 2013;2013:636597.
8. Ravindranath MH, Muthugounder S, Presser N, Viswanathan S. Anticancer therapeutic potential of soy isoflavone, genistein. *Adv Exp Med Biol*. 2004;546:121–165.
9. Goh MJ, Park JS, Bae JH, Kim DH, Kim HK, Na YJ. Effects of orthodihydroxyisoflavone derivatives from Korean fermented soybean paste on melanogenesis in B16 melanoma cells and human skin equivalents. *Phytother Res*. 2012;26(8):1107–1112.
10. US Food & Drug Administration. Waiver of in vivo bioavailability and bioequivalence studies for immediate-release solid oral dosage forms based on a biopharmaceutics classification system. 1005598 FNL [updated 2016 Jun 5]. Available from: www.fda.gov/downloads/drugs/guidancecomplianceregulatoryinformation/guidances/ucm070246.pdf. Accessed April 1, 2016.
11. Baghel S, Cathcart H, O'Reilly NJ. Polymeric amorphous solid dispersions: A review of amorphization, crystallization, stabilization, solid-state characterization, and aqueous solubilization of biopharmaceutical classification system class II drugs. *J Pharm Sci*. 2016;105(9):2527–2544.
12. Vo AQ, Feng X, Pimparade M, et al. Dual-mechanism gastroretentive drug delivery system loaded with an amorphous solid dispersion prepared by hot-melt extrusion. *Eur J Pharm Sci*. 2017;102:71–84.
13. Shah S, Maddineni S, Lu J, Repka MA. Melt extrusion with poorly soluble drugs. *Int J Pharm*. 2013;453(1):233–252.
14. Paudel A, Worku ZA, Meeus J, Guns S, Van den Mooter G. Manufacturing of solid dispersions of poorly water soluble drugs by spray drying: formulation and process considerations. *Int J Pharm*. 2013;453(1):253–284.
15. Greco K, Bogner R. Solution-mediated phase transformation: significance during dissolution and implications for bioavailability. *J Pharm Sci*. 2012;101(9):2996–3018.
16. Van Duong T, Van den Mooter G. The role of the carrier in the formulation of pharmaceutical solid dispersions. Part II: amorphous carriers. *Expert Opin Drug Deliv*. 2016;13(12):1681–1694.
17. Lu Y, Park K. Polymeric micelles and alternative nanonized delivery vehicles for poorly soluble drugs. *Int J Pharm*. 2013;453(1):198–214.
18. Ahmad M, Rai SM, Mahmood A. Hydrogel microparticles as an emerging tool in pharmaceutical field: a review. *Adv Polym Tech*. 2016;35(2):121–128.
19. Ueda K, Higashi K, Moribe K. Application of solid-state NMR relaxometry for characterization and formulation optimization of grinding-induced drug nanoparticle. *Mol Pharm*. 2016;13(3):852–862.
20. Zhang GC, Lin HL, Lin SY. Thermal analysis and FTIR spectral curve-fitting investigation of formation mechanism and stability of indomethacin-saccharin cocrystals via solid-state grinding process. *J Pharm Biomed Anal*. 2012;66:162–169.
21. Muehlenfeld C, Kann B, Windbergs M, Thommes M. Solid dispersion prepared by continuous cogrinding in an air jet mill. *J Pharm Sci*. 2013;102(11):4132–4139.
22. Gupta P, Kakumanu VK, Bansal AK. Stability and solubility of celecoxib-PVP amorphous dispersions: a molecular perspective. *Pharm Res*. 2004;21(10):1762–1769.
23. Goto H, Terao Y, Akai S. Synyhesis of various kinds of isoflavones, isoflavanes, and biphenyl-ketones and their 1,1-diphenyl-2-picrylhydrazyl radical-scavening activities. *Chem Pharm Bull (Tokyo)*. 2009;57(4):346–360.
24. Higuchi T, Connors KA. Phase-solubility techniques. *Adv Anal Chem Instr*. 1965;4:117–122.
25. Lee CW, Lin ZC, Hu SC, et al. Urban particulate matter down-regulates filaggrin via COX2 expression/PGE2 production leading to skin barrier dysfunction. *Sci Rep*. 2016;6:27995.
26. Ahuja M, Dhake AS, Sharma SK, Majumdar DK. Topical ocular delivery of NSAIDs. *AAPS J*. 2008;10(2):229–241.
27. Hu J, Johnston KP, Williams RO 3rd. Nanoparticle engineering processes for enhancing the dissolution rates of poorly water soluble drugs. *Drug Dev Ind Pharm*. 2004;30(3):233–245.
28. Colombo I, Grassi G, Grassi M. Drug mechanochemical activation. *J Pharm Sci*. 2009;98(11):3961–3986.
29. Salazar J, Müller RH, Möschwitzer JP. Performance comparison of two novel combinative particle-size-reduction technologies. *J Pharm Sci*. 2013;102(5):1636–1649.
30. Raval MK, Patel JM, Parikh RK, Sheth NR. Dissolution enhancement of chlorzoxazone using cogrinding technique. *Int J Pharm Investig*. 2015;5(4):247–258.
31. Vaghani SS, Patel MM. pH-sensitive hydrogels based on semi-interpenetrating network (semi-IPN) of chitosan and polyvinyl pyrrolidone for clarithromycin release. *Drug Dev Ind Pharm*. 2011;37(10):1160–1169.
32. Yang C, Xu X, Wang J, An Z. Use of the co-grinding method to enhance the dissolution behavior of a poorly water-soluble drug: generation of solvent-free drug-polymer solid dispersions. *Chem Pharm Bull (Tokyo)*. 2012;60(7):837–845.
33. Sadeghi F, Ashofteh M, Homayouni A, Abbaspour M, Nokhodchi A, Garekani HA. Antisolvent precipitation technique: A very promising approach to crystallize curcumin in presence of polyvinyl pyrrolidon for solubility and dissolution enhancement. *Colloids Surf B Biointerfaces*. 2016;147:258–264.
34. Hwang du H, Kim YI, Cho KH, et al. A novel solid dispersion system for natural product-loaded medicine: silymarin-loaded solid dispersion with enhanced oral bioavailability and hepatoprotective activity. *J Microencapsul*. 2014;31(7):619–626.
35. Khutoryanskiy VV. Hydrogen-bonded interpolymer complexes as materials for pharmaceutical applications. *Int J Pharm*. 2007;334(1–2):15–26.
36. Jog R, Burgess DJ. Pharmaceutical amorphous nanoparticles. *J Pharm Sci*. 2017;106(1):39–65.
37. Jain P, Banga AK. Inhibition of crystallization in drug-in-adhesive-type transdermal patches. *Int J Pharm*. 2010;394(1–2):68–74.
38. Kim KE, Cho D, Park HJ. Air pollution and skin diseases: adverse effects of airborne particulate matter on various skin diseases. *Life Sci*. 2016;152:126–134.
39. Morita A. Tobacco smoke causes premature skin aging. *J Dermatol Sci*. 2007;48(3):169–175.
40. Quan T, Qin Z, Xia W, Shao Y, Voorhees JJ, Fisher GJ. Matrix-degrading metalloproteinases in photoaging. *J Investig Dermatol Symp Proc*. 2009;14(1):20–24.

41. Bosch R, Philips N, Suárez-Pérez JA, et al. Mechanisms of photoaging and cutaneous photocarcinogenesis, and photoprotective strategies with phytochemicals. *Antioxidants (Basel)*. 2015;4(2):248–268.
42. Rennolds J, Malireddy S, Hassan F, et al. Curcumin regulates airway epithelial cell cytokine responses to the pollutant cadmium. *Biochem Biophys Res Commun*. 2012;417(1):256–261.
43. Tsai MH, Hsu LF, Lee CW, et al. Resveratrol inhibits urban particulate matter-induced COX-2/PGE2 release in human fibroblast-like synoviocytes via the inhibition of activation of NADPH oxidase/ROS/NF-κB. *Int J Biochem Cell Biol*. 2017;88:113–123.
44. Loh ZH, Samanta, AK, Heng PWS. Overview of milling techniques for improving the solubility of poorly water-soluble drugs. *Asian J Pharm Sci*. 2015;10(4):255–274.